Inorg. Chem. **2008**, *47*, 8635−8640

Mechanisms of the Water−Gas-Shift Reaction by Iron Pentacarbonyl in the Gas Phase

Xavier Rozanska* and Rodolphe Vuilleumier

Laboratoire de Physique Théorique de la Matière Condensée, UMR 7600 CNRS, Université Pierre et Marie Curie, Paris 6, 4 place Jussieu, F-75005 Paris Cedex, France

Received January 30, 2008

We analyzed the mechanisms of the water−gas-shift reaction catalyzed by $Fe(CO)_5/OH^-$ in the gas phase using DFT methods. The systematic analysis of the accessible reaction mechanisms and the consideration of the Gibbs free energies allows for different reaction routes than previously suggested. In the dominant catalytic cycle, the hydride $[FeH(CO)_4]$- is the important intermediate. Associative reaction mechanisms are not favorable under moderate and low pressures. At high pressure, a side reaction takes over and prevents the conversion of H_2O and CO to H_2 and CO_2 and leads to the formation of HCOOH.

Introduction

The water−gas-shift (WGS) reaction is an important reaction coupled to the Friedel−Craft process and H_2 production according to[1,2]

$$C_nH_{2n+2} + nH_2O = nCO + (2n+1)H_2 \quad (1)$$

$$CO + H_2O = CO_2 + H_2 \quad (2)$$

Several groups investigated the WGS reaction catalyzed by homogeneous catalysts because the $\Delta G_{298}°$, $\Delta H_{298}°$, and $\Delta S_{298}°$ values of eq 2 are −4.76 kcal, 0.68 kcal, and 18.3 cal/deg and −6.82 kcal, −9.84 kcal, and −10.1 cal/deg with water being present as a liquid and with all species being present as gas, respectively.[2−8] The most suitable catalysts appeared to be transition metal complexes in organic solvent (e.g., methanol), in basic or acidic conditions. Among the catalysts for this reaction, iron pentacarbonyl, albeit not the most active catalyst, was selected to extensively analyze the WGS reaction mechanisms experimentally[3,9−12] and theoretically.[13,14] However, a comprehensive and systematic theoretical analysis of the reaction is still missing. The reaction pathways that have been explored using theoretical chemistry methods are indicated in Scheme 1. Several other reaction mechanisms are possible and have not been analyzed so far.

Torrent at al.[13] precisely followed the reaction mechanisms as they have been experimentally suggested (Scheme 1a).[12] In the catalytic cycle in Scheme 1a, $[FeH(CO)_4]^-$ is experimentally observed: this intermediate is the master stone upon which the entire cycle is constructed, and the other intermediates are not experimentally observed. However, the OH^- desorption from the iron complex is very energy demanding (ΔH = 308 kJ/mol in the gas phase) and makes Scheme 1a rather unlikely. We will consider an alternative to this catalytic cycle in which OH^- desorption is not required.

* To whom correspondence should be addressed. E-mail: tgakxr@chem.tue.nl. Fax: +33 4 72 72 88 60. Present address: Laboratoire de Chimie, UMR 5182 CNRS, ENS Lyon, 46 Allée d'Italie, F-69364 Lyon Cedex 7, France.

(1) Ford, P. C. *Acc. Chem. Res.* **1981**, *14*, 31–37.
(2) King, A. D., Jr. ; King, R. B.; Yang, D. B. *J. Am. Chem. Soc.* **1980**, *102*, 1028–1032.
(3) Pearson, R. G.; Mauermann, H. *J. Am. Chem. Soc.* **1982**, *104*, 500–504.
(4) Kang, H.-C.; Mauldin, C. H.; Cole, T.; Slegeir, W.; Cann, K.; Pettit, R. *J. Am. Chem. Soc.* **1977**, *99*, 8323–8325.
(5) Cheng, C.-H.; Hendriksen, D. E.; Eisenberg, R. *J. Am. Chem. Soc.* **1977**, *99*, 2791–2792.
(6) Laine, R. M.; Rinker, R. G.; Ford, P. C. *J. Am. Chem. Soc.* **1977**, *99*, 252–253.
(7) Cheng, C.-H.; Eisenberg, R. *J. Am. Chem. Soc.* **1978**, *100*, 5968–5970.
(8) King, R. B.; Frazier, C. C.; Hanes, R. M.; King, A. D., Jr. *J. Am. Chem. Soc.* **1978**, *100*, 2925–2927.
(9) Lane, K. R.; Lee, R. E.; Sallans, L.; Squires, R. R. *J. Am. Chem. Soc.* **1984**, *106*, 5767–5772.
(10) Lane, K. R.; Sallans, L.; Squires, R. R. *Organometallics* **1985**, *4*, 408–410.
(11) 11 Miller, A. E. S.; Beauchamp, J. L. *J. Am. Chem. Soc.* **1991**, *113*, 8765–8770.
(12) Sunderlin, L. S.; Squires, R. R. *J. Am. Chem. Soc.* **1993**, *115*, 337–343.
(13) Torrent, M.; Solà, M.; Frenking, G. *Organometallics* **1999**, *18*, 2801–2812.
(14) Barrows, S. E. *Inorg. Chem.* **2004**, *43*, 8236–8238.

10.1021/ic8001866 CCC: $40.75
Published on Web 08/29/2008

Scheme 1. Suggested Reaction Mechanisms in the WGS Reaction[12,14]

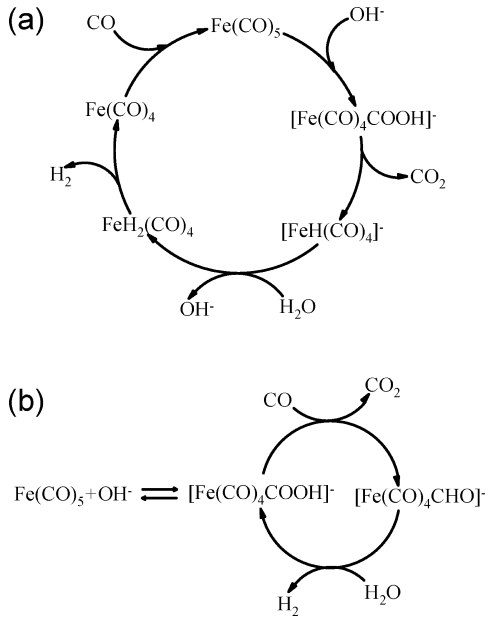

Barrows[14] considered exclusively associative reaction mechanisms with a catalytic cycle where OH^- desorption is not required (Scheme 1b). In this catalytic cycle, $[FeH(CO)_4]^-$ is however not present. The Gibbs free energies of the intermediates and transition structures were not considered, although they are important to predict whether the reaction mechanisms are kinetically favored.

We systematically analyze the gas phase mechanisms of the WGS reaction in basic conditions, including some that have not been considered so far. We have calculated the Gibbs free energies of all structures: the calculations reveal that a different catalytic cycle than those previously proposed is dominant.

Models and Methods

The use of density functional theory (DFT) hybrid methods such as B3LYP[15] or RPBE[16] to describe iron−carbonyl complexes properties was found to give realistic results.[17−22] In the present study, the intermediates and transition structures are analyzed with B3LYP and a triple-ζ plus polarization basis set on all atoms (TZVP)[23] employing Gaussian 98 package.[24] In addition, to pave the way to an analysis of the solvent effect on the reaction, the structures are described with plane wave basis set using the CPMD package.[25] The RPBE functional with an energy cutoff of 120 Ry are chosen for these calculations. The B3LYP structures are used as guess for the RPBE structures calculations. All intermediates and transition structures are characterized by frequency calculations within the rigid-rotor harmonic approximation. We verify that there are none or only one imaginary frequency of vibration for intermediate or transition structure, respectively. Evaluation of the Gibbs free energies, enthalpies, energies corrected from the zero point vibrational energy (E_{ZP}), and reaction rates is done using the standard formalism and equations.[26] Further details concerning the choice of DFT methods and other calculation parameters can be found in the Supporting Information.

Results and Discussion

First, we describe step-by-step the different reaction mechanisms that are possible. We then consider what would be the viable catalytic cycle based on the analysis of the Gibbs free energies of the different intermediates and transition structures. The effect of the pressure on these values is also analyzed.

The details of the structures that are analyzed are reported in Figure 1. The reaction pathways can be seen in the reaction energy diagrams in Figure 2. The E_{ZP} and Gibbs free energies under standard conditions of pressure and temperature are also given in Figure 2.

The adsorption of OH^- to $Fe(CO)_5$ (**1**) is strongly exothermic with a standard enthalpy of −323 kJ/mol and leads to $[Fe(CO)_4COOH]^-$ (**2**). B3LYP/TZVP appears to overestimate this adsorption energy: this overestimation stems from TZVP basis set as can be seen in the Supporting Information (Tables S3 and S4). It occurs when OH^- adsorbs to $Fe(CO)_5$; consecutive energies relative to this compound are basically unchanged regardless of the basis set (Table S6, Supporting Information). It is thus justified to proceed at TZVP level of theory. After **2** is formed, two paths can be followed: CO_2 can be released, which leads to $[FeH(CO)_4]^-$ (**3**), or **2** and CO react together, which leads to $[Fe(CO)_4CHO]^-$ (**4**) and CO_2. The E_{ZP} difference between these two structures is small, but the Gibbs free energy difference is 37 kJ/mol more favorable for **3** + CO + H_2O + CO_2, at standard pressure and temperature. Is this thermodynamically stable product also the kinetic product? TS **2/4a** is the transition structure that connects **2** + CO to **4** + CO_2. Its E_{ZP} is 92 kJ/mol with respect to **2** + CO. TS **2/3** connects **2** to **3** and CO_2 and has a E_{ZP} 30 kJ/mol higher than that of TS **2/4a**. However, the rates of the conversion of **2** to **3** and **4** are given by

$$r_{\mathbf{2}\rightarrow\mathbf{3}} = k_{\mathbf{2}\rightarrow\mathbf{3}}[\mathbf{2}] \quad (3)$$

and

$$r_{\mathbf{2}\rightarrow\mathbf{4a}} = k_{\mathbf{2}\rightarrow\mathbf{4a}}[\mathbf{2}][\mathrm{CO}] \quad (4)$$

respectively, with

$$k_{x\rightarrow y} = \frac{kT}{h}\exp\left(-\frac{\Delta G_{yx}}{RT}\right) \quad (5)$$

where ΔG_{yx} is the Gibbs free energy between the respective transition structure y and intermediate x (Figure 2) and [**2**] and [CO] are the concentrations (or pressures in the gas phase) of **2** and CO, respectively. Hence, the ratio between the rates of formation of **3** and **4** is

(15) (a) Becke, A. D. *J. Chem. Phys.* **1993**, *98*, 5648–5652. (b) Lee, C.; Yang, W.; Parr, R. G. *Phys. Rev. B* **1988**, *37*, 785–789.
(16) Zhang, Y.; Yang, W. *Phys. Rev. Lett.* **1998**, *80*, 890.
(17) McClelland, B. W.; Robiette, A. G.; Hedberg, L.; Hedberg, K. *Inorg. Chem.* **2001**, *40*, 1358–1362.
(18) Lüthi, H. P.; Siegbahn, P. E. M.; Almlöf, J. *J. Phys. Chem.* **1985**, *89*, 2151–2161.
(19) Jonas, V.; Thiel, W. *J. Chem. Phys.* **1995**, *102*, 8474–8484.
(20) Bérces, A.; Ziegler, T. *J. Phys. Chem.* **1995**, *99*, 11417–11423.
(21) Gonzàlez-Blanco, O.; Branchadell, V. *J. Chem. Phys.* **1999**, *110*, 778–783.
(22) Jiang, Y.; Lee, T.; Rose-Petruck, G. R. *J. Phys. Chem. A* **2003**, *107*, 7524–7538.
(23) Schäfer, A.; Huber, C.; Ahlrichs, R. *J. Chem. Phys.* **1994**, *100*, 5829–5835.

$$\frac{r_{2\rightarrow 3}}{r_{2\rightarrow 4a}} = \frac{k_{2\rightarrow 3}}{k_{2\rightarrow 4a}[\mathrm{CO}]} \quad (6)$$

The ratio between $k_{2\rightarrow 3}$ and $k_{2\rightarrow 4a}$ is ∼130 under standard conditions. Therefore, the rate of the conversion of **2** into **3** is large in comparison with the rate of the formation of **4** through TS **2/4a**, unless the concentration of CO is very large. We will consider the effect of the pressure on the Gibbs free energies in a following paragraph.

Let us first consider the reaction pathways that are accessible from **4** + H_2O + CO, which is an important intermediate in the catalytic cycle proposed by Barrows (Scheme 1b). Intermediate **4** can decompose to **3** and CO (TS **3/4a**), which is the product obtained from **2** + CO + H_2O through TS **2/3** + CO + H_2O, or it can react with H_2O following two distinct mechanisms to lead to **2** and H_2 (TS **2/4b**) or to **3** and HCOOH (TS **3/4b**). The formation of

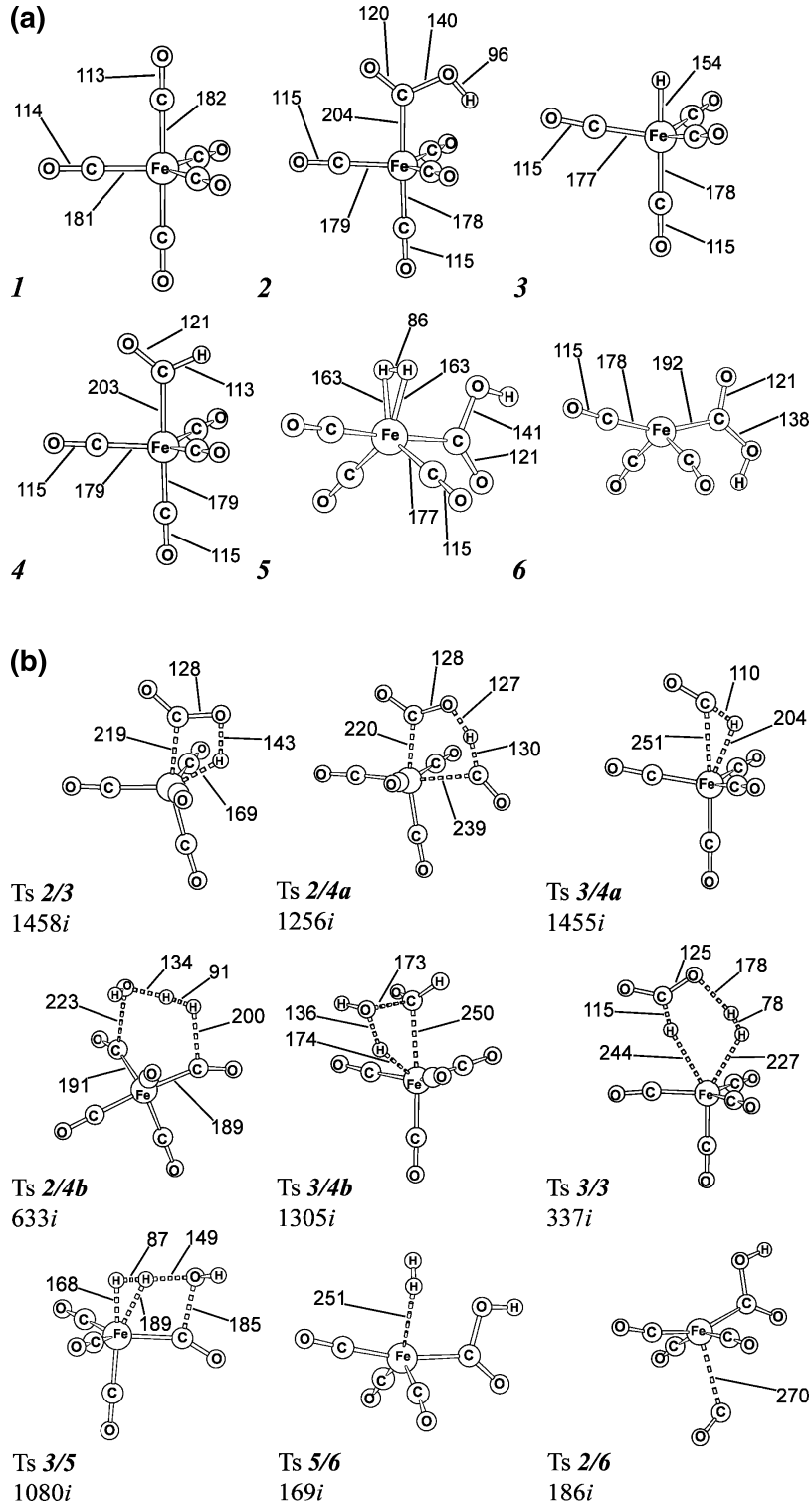

Figure 1. (a) Geometry details of the intermediates in the gas-phase WGS by $Fe(CO)_5/OH^-$ (in pm). (b) Geometry details and imaginary mode values of the transition structures in the gas-phase WGS by $Fe(CO)_5/OH^-$ (in pm and cm^{-1}).

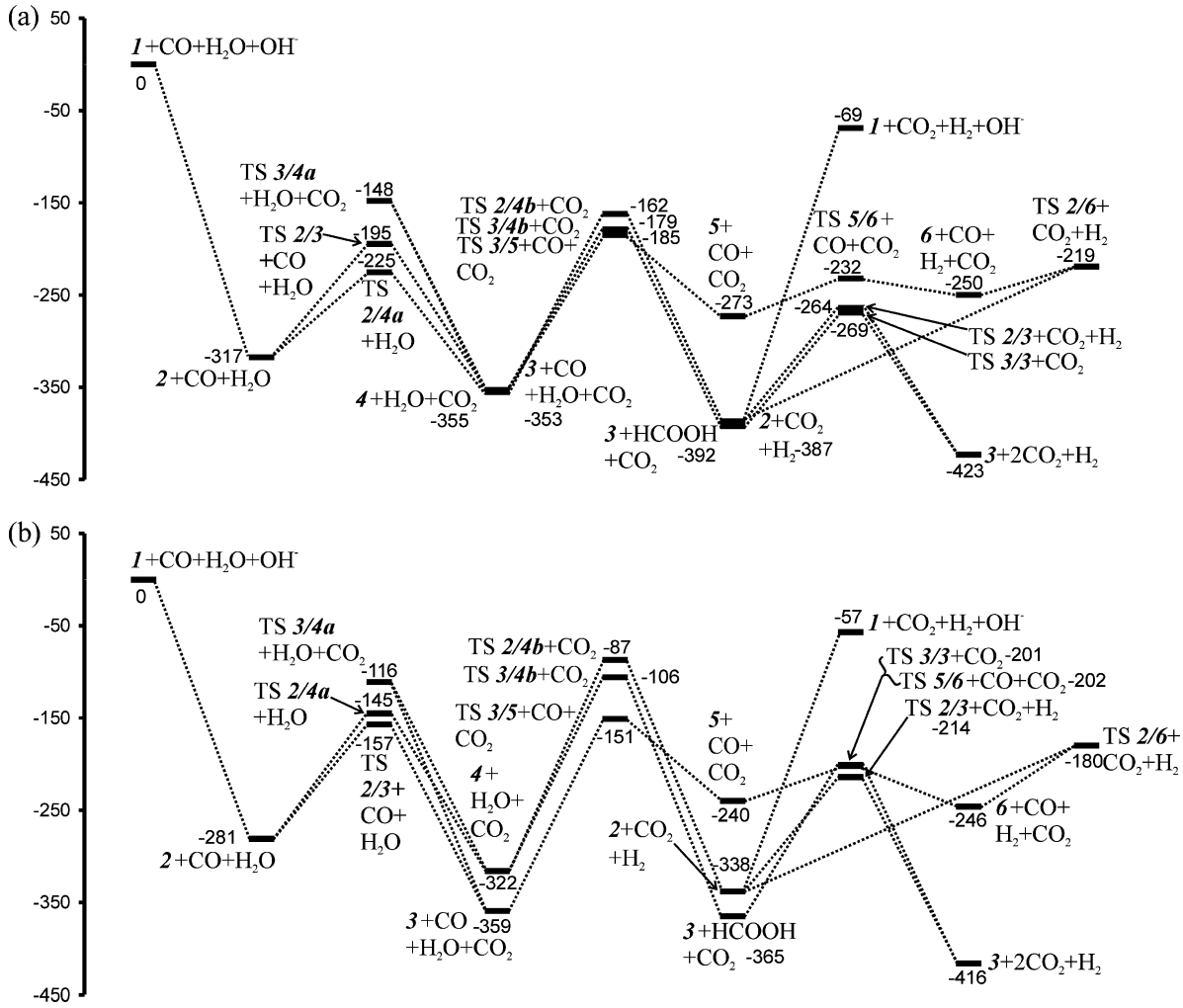

Figure 2. (a) E_{ZP} and (b) Gibbs free energy at 298 K and 1 bar reaction diagrams of the gas-phase WGS by $Fe(CO)_5/OH^-$ (in kJ/mol).

formic acid is not surprising: homogeneous transition metal complex catalysts are known catalysts in the conversion of CO_2 and H_2 to HCOOH.[27] When the Gibbs free energies of the transition structures TS **2/4b** and TS **3/4b** are considered, the conversion of **4** and H_2O into **3** and HCOOH is the fastest and is ~2140 larger than the rate of the conversion of **4** and H_2O into **2** and CO_2 and H_2. TS **2/4b** and TS **3/4b** are the two transition structures that allow the reaction to proceed forward here. The reaction through TS **3/4a** proceeds backward to **3** + CO + H_2O + CO_2. This transition structure has a lower Gibbs free energy under standard conditions than that of TS **2/4b** and TS **3/4b**. Hence, even if the pathway through TS **2/4a** from **2** + CO dominates over the pathway through TS **2/3**, the intermediate **3** will become dominant because of the pathway through TS **3/4a**.

Formic acid can react with **3** through TS **3/3** and transforms into H_2 and CO_2. The energy of the transition structure is 123 kJ/mol with respect to **3** + HCOOH.

Now, we come back to intermediate **3** + CO + H_2O + CO_2 because it is the kinetic and thermodynamic product that is reached from **2** + CO + H_2O. As described before, OH^- adsorbs to $Fe(CO)_5$ to form $[Fe(CO)_4COOH]^-$ complex (**2**), which decomposes into $[FeH(CO)_4]^-$ (**3**) and CO_2 through TS **2/3**. This reaction pathway is experimentally suggested to take place because of the observation of iron hydrides.[8,12] Intermediate **3** can react with water. However, the transition structure of this reaction has not been analyzed so far. Torrent et al.[13] theoretically analyzed the reaction sequence from such iron hydride complex. They based their investigations only on the experimentally suggested pathway (Scheme 1a). Unfortunately, the experimental suggestion is somewhat controversial: it is proposed that $[FeH(CO)_4]^-$

(24) Frisch, M. J.; Trucks, G. W.; Schlegel, H. B.; Scuseria, G. E.; Robb, M. A.; Cheeseman, J. R.; Zakrzewski, V. G.; Montgomery, J. A., Jr.; Stratmann, R. E.; Burant, J. C.; Dapprich, S.; Millam, J. M.; Daniels, A. D.; Kudin, K. N.; Strain, M. C.; Farkas, O.; Tomasi, J.; Barone, V.; Cossi, M.; Cammi, R.; Mennucci, B.; Pomelli, C.; Adamo, C.; Clifford, S.; Ochterski, J.; Petersson, G. A.; Ayala, P. Y.; Cui, Q.; Morokuma, K.; Malick, D. K.; Rabuck, A. D.; Raghavachari, K.; Foresman, J. B.; Cioslowski, J.; Ortiz, J. V.; Stefanov, B. B.; Liu, G.; Liashenko, A.; Piskorz, P.; Komaromi, I.; Gomperts, R.; Martin, R. L.; Fox, D. J.; Keith, T.; Al-Laham, M. A.; Peng, C. Y.; Nanayakkara, A.; Gonzalez, C.; Challacombe, M.; Gill, P. M. W.; Johnson, B. G.; Chen, W.; Wong, M. W.; Andres, J. L.; Head-Gordon, M.; Replogle, E. S.; Pople, J. A. *Gaussian 98*; Gaussian, Inc.: Pittsburgh, PA, 1998.
(25) CPMD, Copyright IBM Corp 1990−2006;Copyright MPI für Festkörperforschung Stuttgart 1997−2001.
(26) Van Santen, R. A.; Niemantsverdriet, J. W. *Chemical Kinetics and Catalysis*, Plenum Press: New York, 1995.
(27) (a) Inoue, Y.; Izumida, H.; Sasaki, Y.; Hashimoto, H. *Chem. Lett.* **1976**, 863–864. (b) The reaction conditions are complex 0.1 mmol, base 50 mmol, water 500 mmol, benzene 10 mL, CO_2 25 atm, and H_2 25 atm.

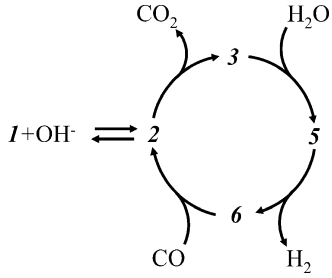

Figure 3. Catalytic cycle in the gas-phase WGS by $Fe(CO)_5/OH^-$.

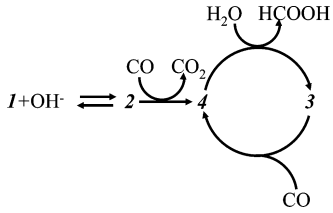

Figure 4. Dominant high-pressure catalytic cycle in the conversion of CO and H_2O by $Fe(CO)_5/OH^-$.

reacts with H_2O, which leads to $FeH_2(CO)_4$ and OH^-. The desorption of OH^- from the iron complex is energetically demanding with theoretical and experimental reaction energies of 308[13] and 301[12] kJ/mol, respectively. Hence, we consider a reaction mechanism that allows the conversion of $[FeH(CO)_4]^-$ and H_2O without OH^- desorption from the iron complex and investigate the transition structure that links intermediate **3** and H_2O to $[FeH_2(CO)_3COOH]^-$ (**5**). The transition structure TS **3/5** is obtained: it has relatively lower zero point corrected and Gibbs free energies (168 and 208 kJ/mol with respect to **3** + H_2O, respectively) than those of TS **2/4b** (193 and 235 kJ/mol with respect to **4** + H_2O, respectively) and TS **3/4b** (176 and 216 kJ/mol with respect to **3** + CO + H_2O, respectively). TS **3/5** has lower relative zero point corrected and Gibbs free energies than TS **3/4a**. Intermediate **5** has rather high energy, but its structure evolves quickly through desorption of H_2 (TS **5/6**) and adsorption of CO (TS **2/6**) to lead to $[Fe(CO)_4COOH]^-$ (**2**). As shown in Figure 2, the energies of the intermediates **5** and **6** + H_2 are relatively high (82 and 105 kJ/mol with respect to **3** + H_2O, respectively), but they remain modest when compared to the reaction energy of ∼300 kJ/mol that is required in the formation of FeH_2CO_4 and OH^-. Furthermore, the barriers in the conversion of **5** to **6** + H_2 and **6** + CO to **2** are very small, and the rates of the conversion of those intermediates into **2** and H_2 and CO_2 are large. Indeed, the Gibbs free energy barrier for TS **5/6** is 38 kJ/mol with respect to **5** at 298 K and 1 bar. It is 66 kJ/mol for TS **2/6** with respect to **6** + CO under the same conditions.

We analyzed the charge distribution in the intermediate and transition state structures, using Mulliken and natural bond charge definitions (Figure S1 in the Supporting Information). The charge analysis confirms that the reaction mechanisms evolve through hydride activation. It can also be observed that the H_2 group of **5** is neutral, forming a true adsorbed hydrogen molecule that is ready for desorption. This is largely confirmed by the geometry analysis of the systems. The H−H distance in **5** is 84 pm, not much greater that the distance of 74 pm in H_2. The H−Fe distance of 163 pm in **5** is stretched from the 154 pm distance in **3**, indicating less H−Fe bonding.

When the reaction mechanisms in the WGS reaction by $Fe(CO)_5/OH^-$ are extensively explored, the experimentally proposed reaction cycle would seem to be unrealistic because of its very high energy requirement (Scheme 1a).[12] A reaction mechanism following the sequence **2** → **4** → **2**[14] is reasonable, but the Gibbs free energies and, hence, reaction rates need to be considered because many other reaction pathways are possible. When this is done, it appears that this sequence is not the one showing the lowest Gibbs free energies and that the catalytic cycle as shown in Figure 3 is the dominant one at standard temperature and pressure.

For a different pressure, P, the Gibbs free energies for any structure can be estimated using

$$\Delta G_{298,P} = RT(N_{\text{struct}} - N_{\text{ref}})\ln(P/P^\circ) \qquad (7)$$

where $\Delta G_{298,P}$ is the Gibbs free energy change with respect to **1** + CO + H_2O + OH^- when pressure goes from P° to P, N_{struct} and N_{ref} are the number of molecular fragments in the considered structure and **1** + CO + H_2O + OH^- (i.e., $N_{\text{ref}} = 4$), respectively. This allows us to analyze the effect of the pressure on the Gibbs free energies and hence on the reaction rates and selectivities between the different reaction routes.

The different intermediates and transition structures in the catalytic cycle in Figure 3 display the largest number of molecular fragments compared to the other possible catalytic cycles (Figure 2 and Scheme 1). Hence, the proposed reaction pathway becomes even more favorable when the pressure is lower than P°. In this catalytic cycle, the dominant species, based on the energies and reaction rates of the elementary reaction steps, is $[FeH(CO)_4]^-$ (**3**) as experimentally observed.

A different catalytic cycle emerges when pressure is high: trivially, high pressure favors associative reaction mechanisms, such as the one proposed by Barrows (Scheme 1b), because this leads to a negative ($N_{\text{struct}} - N_{\text{ref}}$) term. However, a different catalytic cycle appears to become predominant at high pressure when all Gibbs free energies of intermediates and transition structure are considered. In this catalytic cycle, the initiation goes through **1** + OH^- to **2** followed by the conversion of **2** + CO into **4** + CO_2, and the cycle loops between **3** and **4** and converts CO and H_2O into HCOOH (Figure 4). The formation of HCOOH is thermodynamically favorable at high pressure in gas phase. At low pressure, we have seen that HCOOH dissociates into H_2 and CO_2 through TS **3/3**. The experimentally observed iron hydride $[FeH(CO)_4]^-$ (**3**) is part of this cycle. Inoue et al.[27] actually suggested reaction mechanisms that need the presence of organometallic hydrides in their study of catalysts for the CO_2 and H_2 conversion to HCOOH.

Finally, we tested the sensitivity of these results with respect to the DFT method and report the results of the energies for the intermediates and transition structures in Table 1. RPBE energies are lower than B3LYP, with the exception of the intermediates **5** and **6** and transition

Table 1. Zero Point Corrected and Gibbs Free Energy Differences for the Intermediates and Transition Structures Using Different Methods[a]

structure	ΔE_{ZP}	$\Delta\Delta G°$	structure	ΔE_{ZP}	$\Delta\Delta G°$
2 + CO + H_2O	0	0	TS **2/3** + CO + H_2O	−33	−34
3 + CO + H_2O + CO_2	−15	−22	TS **2/4a** + H_2O	−24	−24
4 + H_2O + CO_2	−24	−25	TS **2/4b** + CO_2	−29	−27
2 + CO_2 + H_2	−14	−14	TS **3/4a** + H_2O + CO_2	−56	−56
3 + HCOOH + CO_2	−16	−23	TS **3/4b** + CO_2	−34	−30
5 + CO + CO_2	3	0	TS **3/5** + CO + CO_2	−1	−4
3 + 2CO_2 + H_2	−29	−36	TS **2/3** + CO_2 + H_2	−47	−48
6 + CO + H_2 + CO_2	−1	−4	TS **3/3** + CO_2	−2	5
			TS **5/6** + CO + CO_2	16	14
			TS **2/6** + CO_2 + H_2	15	20

[a] In kJ/mol. The differences are between the RPBE and B3LYP/TZVP values obtained with CPMD and Gaussian 98, respectively.

structures TS **3/3**, TS **3/5**, TS **2/6**, and TS **5/6**. However, the relative ordering of the zero point corrected and Gibbs free energies is not changed for the intermediates and transition structures for RPBE compared to B3LYP. Hence, the catalytic cycles in Figures 3 and 4 are still the dominant ones at low and high pressures, respectively, albeit the rates of reaction are different. B3LYP and RPBE methods appears equally suited to obtain the qualitative description of the selectivity in the reaction mechanism network of the WGS reaction. Further details concerning the effect on the energies when employing a different DFT method can be found in the Supporting Information.

We have analyzed the reaction mechanisms in the gas phase; however this reaction also commonly takes place in the condensed phase. The liquid phase has an energy stabilization effect on the dissociated ion pair intermediates and transition structures.[28] For instance, Amovilli et al.[28] have estimated that the reaction energy of $FeH(CO)_4^- + H_2O = FeH_2(CO)_4 + OH^-$ (Scheme 1a) is ∼200 kJ.mol^{-1} smaller in water solution than in the gas phase, where this reaction is very demanding with $\Delta H = 308$ kJ/mol.[12] However, this stabilization will be smaller in less polar liquids, like methanol, usually used as solvent for the WGS reaction. Furthermore, the stabilization energy by solvent has no reason to be the same on the different intermediates and transition structures along the reaction pathways. Hence, only the calculation and comparison of the rates of all possible reaction pathways described here in explicit solvents can unambiguously suggest which reaction pathways should be favorable in condensed phase.

(28) Amovilli, C.; Floris, F. M.; Solà, M.; Tomasi, J. *Organometallics* **2001**, *20*, 1310–1316.

Conclusions

We analyzed the reaction mechanisms of the WGS reaction by $Fe(CO)_5/OH^-$ in the gas phase using different DFT methods. B3LYP and RPBE similarly suggest the same reaction routes. The Gibbs free energies of the intermediates and transition structures were taken into account to compare the possible routes for the WGS reaction. We have shown the importance of considering Gibbs free energy for studying reaction mechanisms. In the newly proposed dominant catalytic cycles, the hydride $[FeH(CO)_4]^-$ is the important intermediate. The experimentally suggested reaction route, which involves the $Fe(CO)_4$ intermediate, is not realistic because of its high energy requirement. We analyzed also the variations of the Gibbs free energies as a function of pressure. Associative reaction mechanisms as previously suggested are not favorable under moderate and low pressures. At high pressure, a side reaction not leading to the conversion of H_2O and CO to H_2 and CO_2 becomes predominant. This reaction leads to the formation of formic acid. Such reaction has indeed been experimentally observed and is also activated by hydride organometallic complex.[27]

Acknowledgment. This work has been supported by CNRS (SC21/2006). We thank the computing center CCRE of Université Pierre et Marie Curie for the allocated computer time.

Supporting Information Available: Tables S1−S6 with information concerning the choice of DFT methods and other calculation parameters and Figure S1 with Mulliken and natural orbital charges This material is available free of charge via the Internet at http://pubs.acs.org.

IC8001866